MORPHOLOGICAL CLASSIFICATION OF IMPACTS ON THE EURECA & HUBBLE SPACE TELESCOPE SOLAR ARRAYS

M.K. Herbert [†‡] and J.A.M. McDonnell [†]

[†]*Unit for Space Sciences & Astrophysics, University of Kent at Canterbury, Canterbury, Kent CT2 7NT, U.K.*

[‡]*Matra Marconi Space U.K. Ltd P.O. Box 16, Filton, Bristol, BS12 7YB, U.K*

ABSTRACT

Impact morphologies on solar cells may retain vital information to identify impactor origin. Morphology and residue data has not yet been collectively assessed as no morphology classification exists. To this end, nearly 1350 impact images from the EURECA & HST post-flight optical surveys were sorted and classified. Common and unique morphologies were identified on both solar arrays and their stratigraphies interpreted. Unique cumulative flux - size distributions resulted for each morphology. Classes associated with elliptical impacts and front/rear ballistic limits were also identified. Morphology progressions with increasing impact size were observed. This research lays the foundations for a future comparative study with residue data.

1.0 INTRODUCTION

There is a need to establish the extent to which natural and man-made impactors contribute to the low Earth space environment. Retrieval of the EURECA and Hubble Space Telescope (HST) solar arrays (SA) from prolonged exposure in low Earth orbit (LEO) has generated a wealth of impact data which, on careful scrutiny, may assist in satisfying this need. Identifying impactor origin is not an easy task. To date, origin detection is by means of chemical analysis though this does not always produce conclusive results. Further clues as to the size and velocity of the particles responsible for the space impacts may reside with the form, size and characteristic features of the impact site (Ref.1). Given the likelihood that the degree of impact damage is related to impact energy, we ask, to what extent does crater morphology provide a signature of impactor origin? A browse through the wealth of EURECA and HST solar array image data reveals numerous repetitive crater forms and sizes. There are occasions where two unique impacts have almost identical visual appearance. Such consistent and reproducible occurrences of morphology may be of significance and not at all coincidental. This paper presents the foundation work of visually classifying impact morphologies on solar cells to enable future comparison with the corresponding residue data.

2.0 MORPHOLOGY v RESIDUE

Craters formed by space impacts can be considered to possess three basic intrinsic properties; *form*, *size (diameter and depth)* and *residue*. It is probable that such properties constitute the essential nature of the originating particle. Morphology essentially combines *form* and *size*. Therefore, it is not unrealistic to suggest that by analysing impact morphology in conjunction with residue, a fingerprint of the impactor may be revealed. To date, residue analysis has been performed in relative isolation without reference to morphology and therefore, decoding impact damage by this approach has been relatively unexploited.

3.0 AVAILABLE DATA

The full technical output from the EURECA and HST solar array post-flight optical surveys were made available for study (Refs.2-3) comprising high resolution imagery of almost 1350 individual impact sites (Ref.4). These data sets permit a conchoidal diameter range of 130 to 5170μm to be analysed.

4.0 CLASSIFICATION

A simple classification system was devised to group the most common and repeatable impact morphologies. The approach was one of rationalisation, sorting and measurement to produce distinct morphological sets and sub-sets. The entire classification comprised the following sequential processes:

4.1 Filtered Sorting of Impacts

An initial sorting process filtered out less meaningful impacts from the HST and EURECA databases establishing two data sets: *classifiable* and *non-classifiable* impacts. A non-classifiable impact is one which exhibits:

- partial morphology {PM} (ie.straddling a cell edge)
- non-glass impact {NG} (ie. an impact on a buffer or substrate)
- indeterminate morphology {ID} (ie. extreme damage curtailing recognition)

Discarding less meaningful data focused efforts on the classifiable impacts with improved decoding potential.

4.2 Front-Rear Impact Phenomenon Sorting

The classifiable impacts were categorised into front and rear incident morphologies. The definitions of Front-Rear impact phenomenon applied during the HST post-flight analysis were maintained (Ref.3). The impact phenomena relevant to this research were:

- *Front-Top Impact*: damage on the front (glass) face caused by an impact from the same face
- *Front-Back Impact*: damage on the front (glass) face caused by an impact from the rear (substrate) face
- *Rear-Back Impact*: damage on the rear (substrate) face caused by an impact from the front (glass) face

By definition, both Front-Back and Rear-Back impacts are penetrative impact phenomena.

4.3 Shape Sorting of Impacts

The classifiable front and rear incident morphologies were visually categorised into fundamental shape, namely *near-circular* and *elliptical* impacts.

4.4 Sorting by Visual Similarity

Near-circular and elliptical morphologies were classified into distinct groups/sub-groups on the basis of visual similarity. An assessment as to the degree of damage was performed for the following damage zones: *pit* or *hole*, *shatter*, *conchoidal* or *spallation*, *maximum damage*. For each damage zone, visual sorting was performed by matching the following impact criteria: *position, shape, colour, albedo/contrast/lustre, texture/surface finish, cover glass transparency and distinguishing features (halos, cracks etc.)*

4.5 Measurement

Various impact parameters from the visually sorted data {to include pit diameter (Dp) and conchoidal diameter (Dco)} were directly measured from enlarged colour hardcopies of the high resolution images using a steel scale calibrated to 0.5mm. This method permitted a more convenient approach to crater measurement enabling a greater sample of images to be processed. The reliability of this measurement method has been verified (Ref.5). Parameter measurements were recorded in a spreadsheet database so that each class could be characterised by size as well as form. An independent assessment of post-flight impact measurements (Ref.5) has shown Dp to be highly unreliable as the precise extent of the pit was not able to be defined. However, Dco was shown to be extremely well defined and highly reliable. Thus, Dco is the impact size parameter applied throughout this research. Extensive measurement of Front-Back impact data was not performed during this research.

5.0 RESULTS & ANALYSIS

5.1 Morphology Classifications

Comprehensive results of morphology classifications and their images has been published (Ref.6). A breakdown summary of the resultant classifications is presented in Table 5-1:

		Non Classifiable Impacts			Classifiable Impacts											
					Front-Incident (Front-Top)							Rear-Incident (Front-Back)				
					Near-Circular						Ellp	Near-Circular				Ellp
		PM	NG	ID	O	Pre-I	I	II	III	IV	I/II	Pre-A	A	B	C	
SPACECRAFT	EURECA	30	18	45	62	209	66	68	75	56	115	0	0	0	1	0
		93			536							1				
					651							1				
					652											
		745														
	HST	43	5	70	0	0	12	60	80	65	47	11	77	91	43	0
		118			217							222				
					264							222				
					486											
		604														

Table 5-1: Summary of Resultant Morphology Classifications

5.1.1 HST Front-Top Impacts

From 264 classifiable Front-Top impacts, 4 unique classes were observed on the HST SA identified as Class I, II, III & IV. Almost one fifth of the data set demonstrated pronounced ellipticity, prevalent at the smaller size of impact only (Class I & II).

5.1.2 HST Front-Back Impacts

From 222 classifiable Front-Back impacts, 4 unique classes were observed on the HST SA identified as Class Pre-A, A, B & C. None of these showed pronounced signs of ellipticity.

5.1.3 EURECA Front-Top Impacts

From 651 classifiable Front-Top impacts, 6 unique classes were observed on the EURECA solar array identified as Class O, Pre-I, I, II, III & IV. Classes I to IV inclusive matched the morphologies observed on the HST SA. Classes Pre-I, II & III demonstrated further sub-groups. Again, almost one fifth of the data set showed pronounced ellipticity for the smaller size regime (Classes O, Pre-I, I and II).

5.1.4 EURECA Front-Back Impacts

A single classifiable Front-Back impact was observed on the EURECA solar array of Class C morphology.

5.2 Relative Proportions of Classes

The relative proportions of the Front-Top morphology classes observed on both the HST & EURECA are represented in Figures 5-1 and 5-2 respectively.

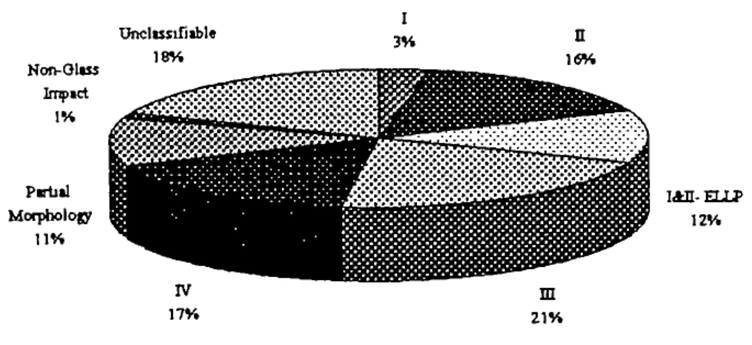

Figure 5-1: HST Front-Top Morphologies - Relative Proportions of Classes

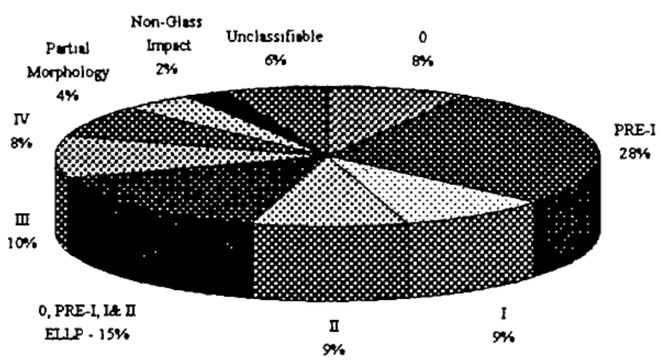

Figure 5-2: EURECA Front-Top Morphologies - Relative Proportions of Classes

On comparison, the significant findings drawn are:

- a relatively high proportion of Class O and Pre-I impacts were only observed on EURECA.
- the proportionate sum of Class I & II impacts for each spacecraft were comparable.
- the proportion of ellipticals were comparable and shared common classes at the smaller crater size.
- the proportions of Class III & IV impacts on HST were much higher than on EURECA.
- HST dataset had a higher proportion of non-classifiable impacts.

5.3 Class - Size Comparison

A comparison of the Front-Top impact sizes for each spacecraft and class is presented in Table 5-2; in general, good correlation between EURECA and HST diametrical measurements were obtained.

Class	Conchoidal Diameter (Dco) [mm]					
	EURECA			HST		
	min	mean	max	min	mean	max
O	0.13	0.37	0.55	N/A	N/A	N/A
Pre-I	0.51	0.66	1.13	N/A	N/A	N/A
I	0.61	0.91	1.34	0.78	1.03	1.21
II	0.67	1.07	1.86	0.94	1.10	1.56
III	0.91	2.01	2.54	1.22	1.82	2.38
IV	1.37	2.31	4.33	1.89	2.38	2.97

Table 5-2: Comparison of Front-Top Measurements

5.4 Class Frequency with Size

The frequency distribution of each Front-Top morphology class was plotted as a function of an impact size parameter. For direct comparison, Figure 5-3 mirrors the frequency - size distributions for EURECA and HST.

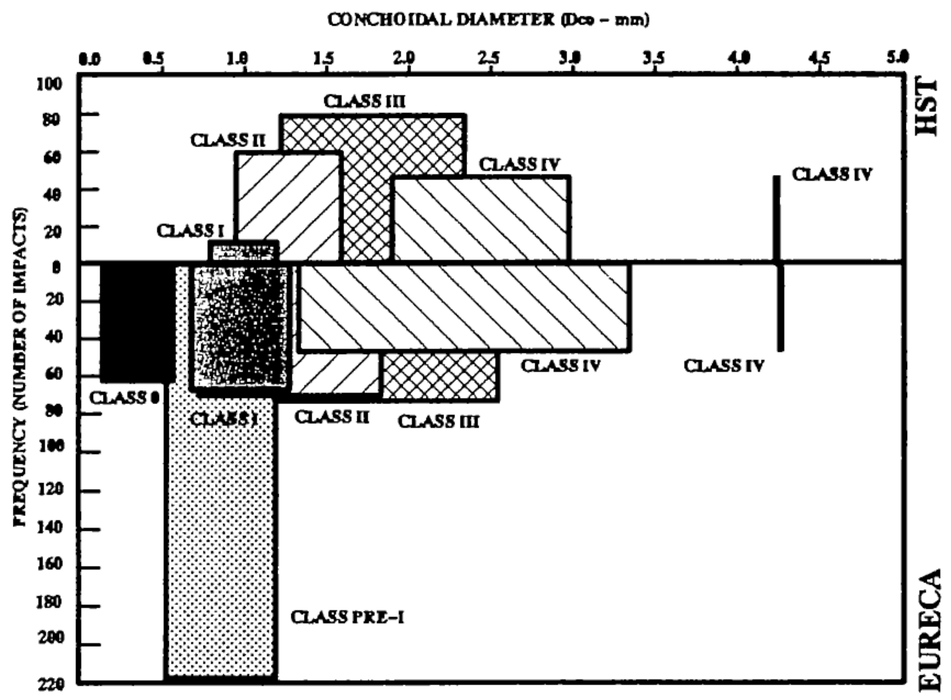

Figure 5-3: EURECA/HST Front-Top Morphologies - Frequency - Size Distributions

Examination and comparison of each distribution highlights a number of significant findings:

- EURECA displays a high quantity of relatively small size impacts (ie. Class O & Pre-I).
- size regimes for each class compare favourably for both EURECA & HST, though the EURECA dataset broadens the size range for most classes.
- discontinuity observed in both EURECA & HST Class IV size distributions ($3.4 \leq Dco \geq 4.3mm$).

5.5 Penetrative Impacts

The threshold at which an incident particle just penetrates a solar cell (usually termed Fmax) is a critical boundary condition in the determination of the target material's ballistic limit. Information relating to ballistic limit was obtained by matching (or pairing) Front to Rear impacts. Such penetrative impacts (termed Rear-Backs) was identified in the HST post-flight data base (Ref.4). Further analysis of the Rear-Back impact phenomena has been performed to determine the most frequent morphology class and associated size regimes.

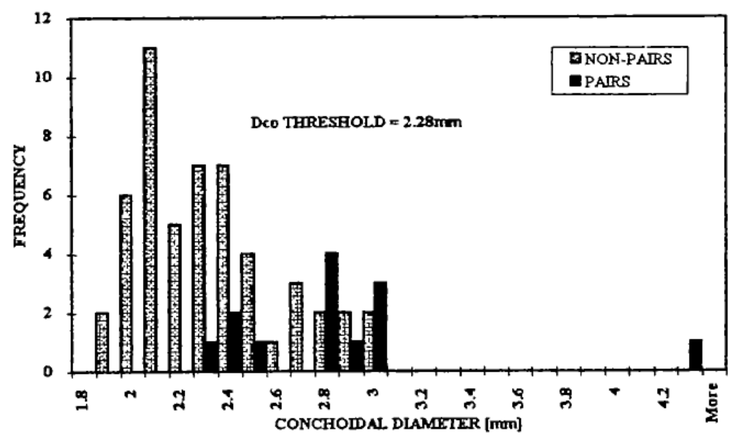

Figure 5-4: Class IV Frequency - Size Distribution

It was found that the incident particle exceeds the target material ballistic limit at the relatively larger Class IV Dco size range. Figure 5-4 shows the resultant frequency - size distribution for the HST Class IV Rear-Back impacts. It is concluded that the Rear-Back phenomena is:

- associated with the HST dataset only
- observed in a Class IV morphology only
- is evident at a Dco size greater than 2.28mm

Note the discontinuity of the paired data in the range ($2.6 \leq Dco \geq 2.8mm$); the reason for this gap in the data is uncertain at this time. However, one possible explanation may be that not all Rear-Back impacts were identified during the rear scanning stage of the post-flight investigation. Further rear scanning may assist in establishing this as the case.

6.0 INTERPRETATION ON MORPHOLOGY

The stratigraphy (or impact growth through the target layers) has been decoded by interpreting each morphology class. These data may be beneficial in hypothesising the dynamics and evolution of impacts in solar cells and assist in understanding the mechanisms by which conchoidal fracturing and spallation occurs.

6.1 Common Morphologies

Common morphology classes are those which have been observed on both the EURECA & HST solar arrays potentially demonstrating 'universal' existence.

6.1.1 Front-Top Impacts

6.1.1.1 Class I

Class I (Fig. 6-1) was the smallest common morphology. The interpretation is based on the classical small crater section in cover glass depicted in (Ref.7). It is typically characterised by a dark central pit (Dpit) around which encircles a prominent halo feature equidistant from its centre and of a constant diameter (Dhalo). A strong photometric contrast exists between the halo and the surrounding plateau or golden yellow shatter zone.

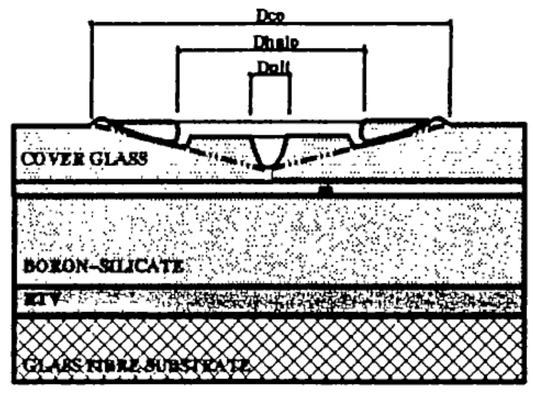

Figure 6-1: Class I Morphology

The impact damage resides in the cover glass only, as continuity of the solar cell electrode was observed within the full extent of the impact zone. A propagating shock wave may cause secondary conchoidal or spallation damage at the outer limits of the impact (Dco) comprising finely shattered cover glass.

6.1.1.2 Class II

Class II (similar to that in Fig. 6-1) was the second smallest common morphology. The significant difference between Class I & II was the development of a narrow blue/cyan spall at the outer fringe of the conchoidal rim. Consequently, the spall and shatter zone became narrowly interspaced by an 'undisturbed' region. Thus, there is evidence to support a Class I to

II progression in which the conchoidal fracture damage becomes larger with increasing impactor energy.

6.1.1.3 Class III

Class III (Fig 6-3) was the second largest common front-top morphology. The damage is no longer only associated with the cover glass layer; the impact penetrates beyond the RTV layer and possibly into the substrate. The dark central pit (Dpit), bound by a re-solidified silicon lip or melt (Dmelt) showed occasional evidence of scorched RTV around the periphery of some pits. The pit walls lined with silicon show evidence of terracing. On occasions where it traversed the melt region, the solar cell electrode was often no longer visible indicating penetration into the silicon layer.

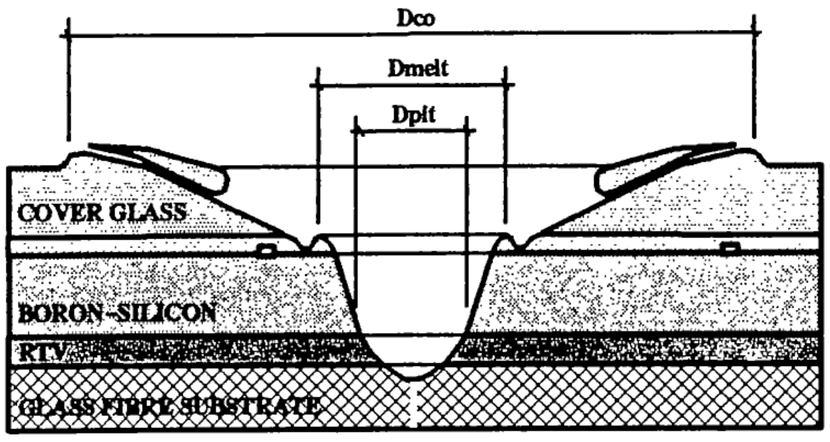

Figure 6-3: Class III Morphology

Beyond the central pit and melt features, lay the conchoidal fracture zone (Dco) comprising blue/cyan annular spall; initially observed in Class II, the spall had significantly developed to a much wider feature suggesting morphology progression from Class II to III. Again, the spallation zone was interspaced by an irregularly profiled 'undisturbed' region.

6.1.1.4 Class IV

Class IV (Fig 6-4) was the largest common front-top morphology. The impact potentially produces a hole through the cell structure (Dhole), bound by a dark scorched region which shows evidence of torn substrate fibres at its base. As with Class III, the melt features (Dmelt) remain. Within the conchoidal fracture zone (Dco), the wide blue/cyan annular spall, consistently observed in Class III, has been reduced to a narrow band interspaced by concentric 'undisturbed' regions on inboard and outboard sides. Beyond the outboard 'undisturbed' region, a yellow outer halo forms from which many radial cracks propagate. These 'undisturbed' regions, also observed on Class II and III, may signify the number of interface layers penetrated by the primary impactor. As the particle penetrates each interface layer, multiple shock waves associated with the conchoidal fracturing process initiate increasingly larger diameter 'undisturbed' rings. Can it be as simple as 'counting' rings? Class IV is the final stage in the progressive development of Front-Top impacts on solar cells.

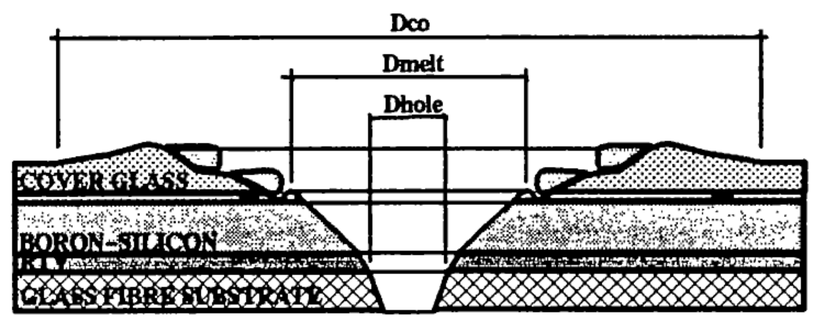

Figure 6-4: Class IV Morphology

6.1.2 Front-Back Impacts

6.1.2.1 Class C

Class C (shown in Fig. 6-5) was the only Front-Back morphology common to both EURECA & HST solar arrays. The impact produces a hole through the entire cell structure (Dhole) around which is an exposed layer of RTV (Drtv). These features are bound by a silicon lined crater wall (Dis) which has a terraced appearance. Finally, outer spall (Dos) comprising finely shattered glass surrounds the crater wall.

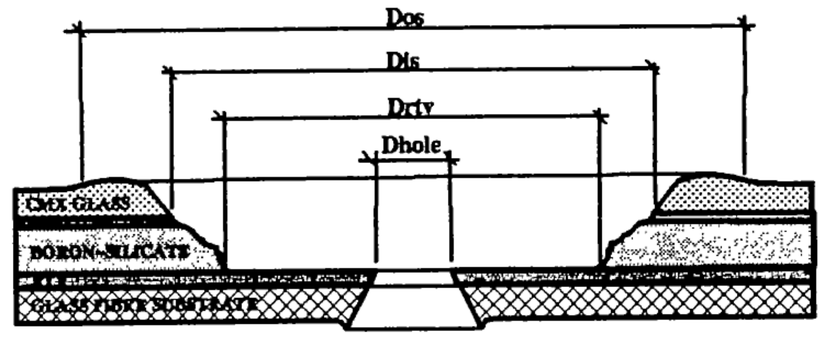

Figure 6-5: Class C Morphology

Often attributed to a 'thin' array construction, this morphology was only expected to occur on the HST SA. However, this study identified one such event on EURECA; this was the largest impact event found on the spacecraft.

6.2 Uncommon Morphologies

Uncommon morphology classes are those which have been observed on either the EURECA or HST SA. Such morphologies may show unique characteristics depending on the construction and thickness of the solar array.

6.2.1 Front-Top Impacts

6.2.1.1 Class O

Class O, the smallest morphology detected on either solar array, was only evident on EURECA. Due to its

very small size, the morphology was extremely difficult to characterise and features were virtually impossible to measure except the largest visible diameter (termed conchoidal). There may have been a pit marked by a very small dark central feature. Otherwise, the class was void of distinguishable features and often irregular in profile. It is fairly certain that the impact damage only resides in the cover glass. Furthermore, the speck-like size range may identify the Pre-I morphology as a potential secondary ejecta candidate.

6.2.1.2 Class Pre-I

Class Pre-I was the most abundant morphology observed on either solar array though only evident on the EURECA. These represented almost two-fifths of the classifiable near-circular impacts. The Pre-I impact features are similar to Class I but distinctly smaller. The morphology is typically characterised by a dark central pit, surrounded by a white/yellow shatter zone and bound by a blue/grey outer spallation zone. Stratigraphy is similar to Class I. Both high quantities and small size range identify the Pre-I morphology as another potential ejecta candidate.

6.2.2 Front-Back Impacts

6.2.2.1 Class Pre-A

Class Pre-A was only evident on the HST solar array. The morphology is characterised by an irregular spallation zone which is crimson edged and raised slightly from the undisturbed surface. No central hole or radial cracking is visible. The Pre-A marks the threshold at which a rear-incident particle is on the verge of penetrating the solar cell.

6.2.2.2 Class A

Class A (Fig.6-6) was only observed on the HST solar array. The morphology is characterised by a central hole through a retained and raised cover glass (Dhole). The retained cover glass has radial cracks bound by an annular spall (Dis and Dos). The crack in the raised cover glass is most likely to have been initiated by lifting of the deformed silicon beneath.

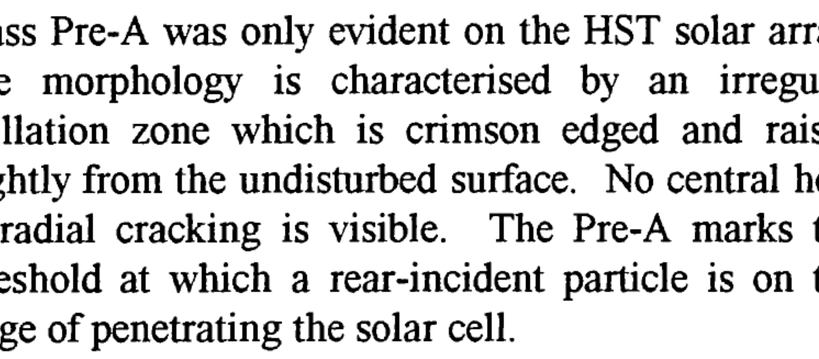

Figure 6-6: Class A Morphology

6.2.2.3 Class B

Class B (Fig.6-7) was only observed on the HST solar array. The morphology is characterised by a central silicon protrusion (Dpro) which evolves from the silicon layer, through which a hole (Dhole) can sometimes be observed. Occasionally, part of the cover glass is not always thrown off indicating that there is a potential progression between Class A and B. Usually, the cover glass is not retained. Class C morphology is perhaps a progression from Class B; the central protrusion 'necks' so that at a critical size it fractures at the RTV interface and is displaced exposing the RTV. The inner silicon wall of the crater appears excavated (Dis) and is surrounded by outer spall in the cover glass (Dos).

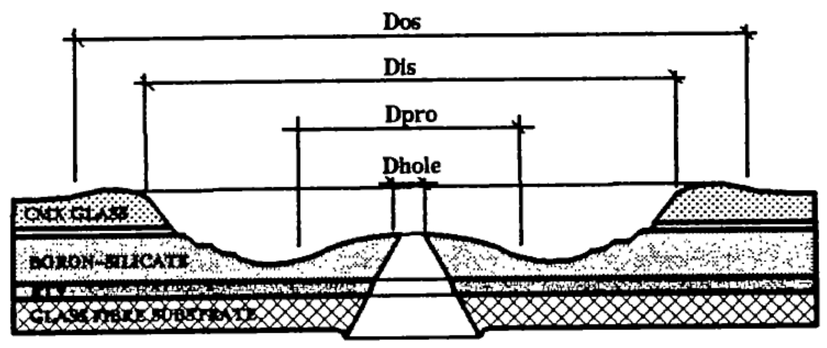

Figure 6-7: Class B Morphology

7.0 CUMULATIVE FLUX

The cumulative flux - size distribution for each Front-Top morphology on the HST and EURECA solar arrays has been produced (Figs 7-1 & 7-2). The flux refers to the impacts whose conchoidal diameter are greater than a certain size. A unique set of flux curves result, each curve representing a morphology class. In the case of EURECA, all sub-groups have been unified. On collective examination, we find that:

- 3 distinct non-overlapping flux - size bands were evident, namely: *Band-1*: Class O; *Band-2*: Class Pre-I, I & II; *Band-3*: Class III & IV.

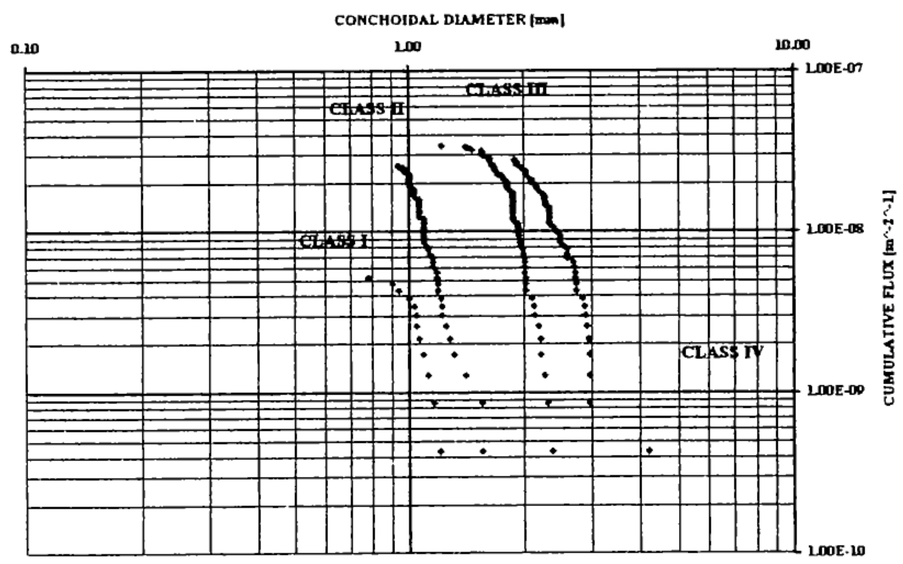

Figure 7-1: HST Cumulative Flux - Size Distribution

- common morphologies: EURECA fluxes are consistently larger than HST; up to 3 times for Classes II, III & IV and 10 times for Class I.
- uncommon morphologies: Class Pre-I generates higher flux levels than Class O by at least 25 times and closely follows and extends the Class I curve.

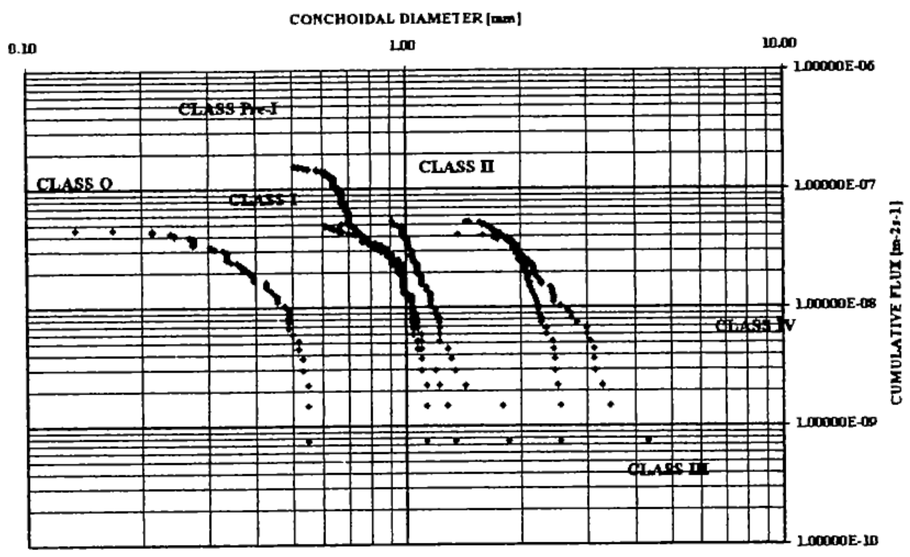

Figure 7-2: EURECA Cumulative Flux - Size Distribution

The full meaning of the distributions may not become apparent until such time that these are assessed in conjunction with known impact origins.

8.0 CONCLUSIONS & RECOMMENDATIONS

The conclusions and recommendations resulting from the classification of morphologies on solar cells are:

- common morphologies: 4 classes of Front-Top impact (I, II, III & IV) and 1 class of Front-Back impact (C) were identified.
- uncommon morphologies: 2 classes of Front-Top impact (O & Pre-I) and 3 classes of Front-Back impact (Pre-A, A & B) were identified. Classes O & Pre-I are potentially secondary ejecta candidates.
- pronounced elliptical impacts can only be visually detected at the smaller size of impact.
- classification has identified the class and size which mark the front and rear incident ballistic limits; Class IV & Pre-A respectively.
- Front-Top & Front-Back morphology progressions with increasing impact size may exist.
- morphologies may provide a useful comparitor or 'bench mark' for future impact modelling (both experimental and simulation).
- unique cumulative flux - size distributions result for each morphology producing distinct non-overlapping class bands.
- morphologies may retain significant information relating to size, velocity and origin of the incident particle; deciphering this information may only be achieved by considering morphology in conjunction with residue.

9.0 RESIDUE DATA COMPARISON

The next stage of this research will take place under ESA Contract 11887/96/NL/JG in which the results from all solar cell residue analyses are being collated and reviewed (Refs. 8-14). Later, morphology and residue for common impact sites will be identified and compared. Only then will it be possible to state whether morphology is a useful indicator of meteoroid and space debris impact damage.

10.0 ACKNOWLEDGEMENTS

Special thanks to Dr W.C. Carey of SAS (B) for his assistance and contribution to this research.

11.0 REFERENCES

1. Grady, M.M., Wright, I.P., '*Space Invaders*', Microscopy & Analysis, July 1996

2. McDonnell, J.A.M., '*EURECA Meteoroid and Debris Post Flight Investigation - Final Report*', ESA Contract Report 10522/93/NL/JG, 1994

3. Carey, W.C., '*Hubble Space Telescope Meteoroid and Debris Post Flight Analysis - Final Report*', ESA Contract Report 10830/94/NL/JG, 1995

4. Unispace Kent, '*HST and EURECA Meteoroid and Debris PFA Results*' - CD-ROM, ESA Contract 11887/96/NL/JG, 1996

5. Carey, W.C., '*MDFEM WP1- Analysis of Impact Data from Optical Surveys - Technical Note*', ESA Contract 11887/96/NL/JG, SAS-MADFEM-TN-001-97, 1997

6. Herbert, M.K., '*WP1- Analysis of Impact Data from Optical Surveys - Technical Note*', ESA Contract 11887/96/NL/JG, MMB-TN-MDFEM-WP1, 1997

7. Mandeville, J.C., Rival, M., '*Small Craters and X-Ray Analysis on HST Solar Cells : Preliminary Results*', Proceedings of the HST Solar Array Workshop, ESA WPP-77, 1995

8. Mandeville, J.C., Rival, M. & Durin, C.,'*HST Solar Panels Hypervelocity Impacts Study Data Organisation*', CNES (F), 1996

9. Wright, I., Sexton, A., Grady, M., '*Impacts into HST Solar Array Panels: Optical Characterisation of Impact Damage and Chemical Analysis of Residues*', Open University, (U.K.), 1996

10. Stephen, T., Jessberger, E & Bischoff, A., '*Hubble Space Telescope Solar Array Microparticulate Impact Analysis*', Max Planck Institut, Heidelberg (G), 1996

11. Borg, J., Fieni, C. & Vassent, B., '*Impact Craters Investigation in HST Solar Arrays*', Institut d'Astrophysique Spatiale, Orsay (F), 1996

12. Heiss, C., Stadermann, F., '*Chemical Analysis of Hypervelocity Impacts on Solar Cells from the Hubble Space Telescope*', Technical University of Darmstadt (G), 1996

13. Endress, M. & Bischoff, A., '*Impacts on Solar Cells and Buffer Samples of the HST Solar Arrays*', University of Muenster (G), 1996

14. Kloeck, W. & Westphal, T., '*Catalogue of Impact Craters on Samples from Solar Arrays of the Hubble Space Telescope*', University of Halle (G), 1996